A Study of Sprinkler Activation for Waffle Beam Structure by Using Fire Dynamic Simulation

Teradej Pongpichaiudom[1], Tanet Aroonsrisopon[2] and Nathasak Boonmee[3]

[1]Fire Protection Engineering, Factory of Engineering, Kasetsart University, teradej.p@ku.th

[2]Department of Mechanical Engineering, Faculty of Engineering, Kasetsart University, tanet.a@ku.ac.th

[3]Department of Mechanical Engineering, Faculty of Engineering, Kasetsart University, fengnab@ku.ac.th

----

ABSTRACT

This research aims to study the responsiveness of the ceiling sprinklers installation in perpendicular beam pattern or waffle slab structure using fire dynamic simulator (FDS) or Computational Fluid Dynamics (CFD) model. The researcher focuses on three major influences to analyze the sprinkler activation time including (1) heat release rate (2) sprinkler distance below ceiling positioning and (3) the sprinkler Response Time Index (RTI). In this research, the researcher chose to scope only one characteristic of waffle slab structure from the actual case. The simulation domain is limited to nine ceiling pockets sizing of 3.4 meter x 1.65 meter. The ceiling height (H) is 9 meters and beam depth (h_b) of 1.15 meter. In addition, the steady state ceiling jet that driven the automatic sprinkler activation are studied coupled with the theoretical correlation to explain smoke behavior in related to the specific ceiling pattern. The result shows that increasing of heat release rate or decreasing sprinkler RTI has rapid the activation of sprinkler whereas the sprinkler distance below ceiling factor generally extends the sprinkler response time in respect of limited heat release rate of 2,400 kW. The characteristic of the smoke plume acts as confined ceiling jet at Radius over Height (R/H) > 0.34 in terms of temperature and R/H > 0.11 in terms of gas velocity.

Keywords: Sprinkler Activation Time, Fire Dynamic Simulator, Computational Fluid Dynamics, Waffle Slab Structure, Steady State Ceiling Jet

1. Introduction

To extinguish fire, water discharge from automatic sprinkler head generally created in the umbrella-shape, providing the design water density and coverage protection area. Much case that the system required up to 12-25 sprinkler heads to give sufficient extinguishing water to control or suppress fire, by that, water pattern for each sprinkler should form perfect discharge shape as practical as engineering solution. The application of automatic sprinkler design and installation has been studied for years, by many international well-known institute, society, or association for example National Fire Protection Association (NFPA) standard which is globally recognized. The solution of sprinkler pattern obstruction are generally mandate in those standards. The researcher sees the challenge when many obstructions has present in actual site and the system installation can be economically explain its performance by fire modelling study.

There are many different type of fire sprinkler in this world. Focusing only the sprinkler head, it is categorized by various factor for example distribution pattern, K-factor, heat sensitive material, response type, and more. Somehow many distributor produces sprinkler head to fit with conditions by combination factors and creates group line of products. One factor that related to the responsiveness of sprinkler is response time index (RTI). Dyer (2008) has simplified the type of sprinkler into three types by sprinkler RTI in $m^{1/2}.s^{1/2}$ unit (1) Fast Response or Quick Response (QR) for RTI value of 50 or less (2) Intermediate Response for RTI value of 50 to 80 and (3) Standard Response (SR) for RTI value 80 or more.

In addition, other significant factors to sprinkler responsiveness includes the positioning of the sprinkler head and heat release rate. By nature of spreading of smoke, we can predict that the smoke will rise and form layer at the ceiling. When automatic sprinkler is installed at ceiling layer, it absorbs heat energy from hot smoke and eventually activates at the point of sufficient temperature. The smoke that form a shallow layer beneath the ceiling surface that carry heat from the fire position is known as ceiling jet.

1.1 Ceiling jet smoke temperature and velocity theory

Boonmee (2016) describes two types of ceiling jet.

1. Unconfined ceiling jet: smoke spreading at ceiling layer is uniform in profile without obstruction intervention. (Johansson et al., 2013) expressed the simple ceiling jet for unconfined condition that the maximum thickness and maximum temperature of the total room is expected at of about 5%-13% and 1%, respectively. The correlation to quantify the maximum gas temperature and velocity at a given position in the ceiling jet flow produced by steady fire developed by Alpert are:

$$\Delta T_{cj}=\frac{16.9\dot{Q}^{2/3}}{H^{5/3}} \qquad \text{When } R/H < 0.18 \qquad (1)$$

$$\Delta T_{cj}=\frac{5.38\left(\frac{\dot{Q}}{R}\right)^{2/3}}{H} \qquad \text{When } R/H > 0.18 \qquad (2)$$

$$\Delta T_{cj}=T_{cj}-T_{\infty} \qquad (3)$$

And

$$u_{cj}= 0.96\left(\frac{Q}{H}\right)^{1/3} \qquad \text{When } R/H < 0.15 \qquad (4)$$

$$u_{cj}=\frac{0.195\dot{Q}^{1/3}H^{1/2}}{R^{5/6}} \qquad \text{When } R/H < 0.15 \qquad (5)$$

Where T_{cj} = ceiling jet temperature (°C or K), T_{∞} = Ambient temperature (°C or K), u_{cj}= ceiling jet velocity (m/s), R = given distance from the center of flame (m), H = room height (m), and $\dot{Q}$ = heat release rate of the fire source (kW)

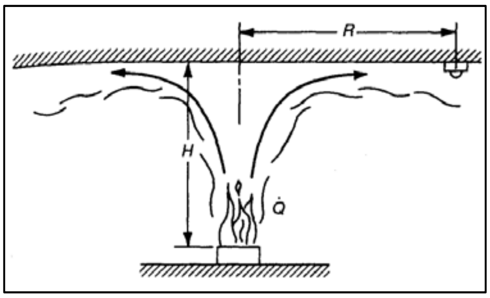

Figure 1 Ceiling jet flow beneath an unconfined ceiling (David)

2. Confined ceiling jet: smoke spreading at ceiling layer faces obstruction such as beam or fixed object which interfere spreading. When beam spacing or width (W) over room height (H) is in range between 0.4 and 1.2, the temperature and smoke velocity correlation for confined ceiling jet can be described by Delichatsios as follows.

$$\frac{\Delta T_{cj}}{\Delta T_0} = 0.37\,(H/W)^{1/3}\exp\left[-0.16\left(\frac{L}{H}\right)\left(\frac{W}{H}\right)^{1/3}\right] \quad (6)$$

$$\Delta T_{cj}=T_{cj}-T_{\infty} \quad (7)$$

$$\frac{u_{cj}}{u_0} = \frac{0.27}{(W/H)^{1/3}} \quad (8)$$

Where T_{cj} = ceiling jet temperature (°C or K), T_{∞} = Ambient temperature (°C or K), ΔT_0 = the different value between plume centerline temperature and ambient temperature (°C or K), H = room height (m), W = beam spacing or width (m), L = reference distance from the heat source (m), u_{cj}= ceiling jet velocity (m/s), u_0= ceiling jet velocity at plume centerline (m/s)

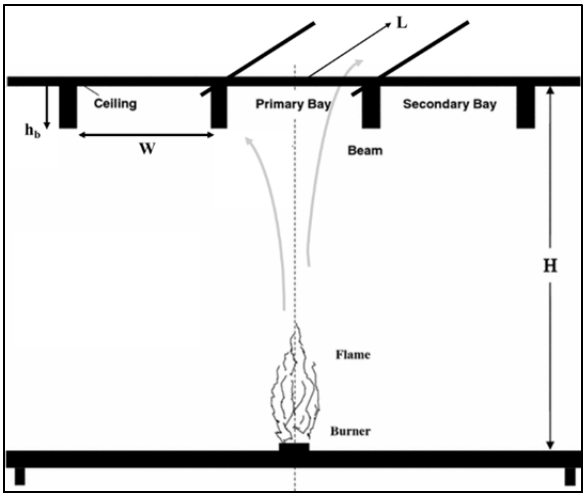

Figure 2 Ceiling jet flow beneath a confined ceiling.

From the equation (6) and (8), the term of smoke plume temperature (T_0) and plume velocity (u_0) at height z can be determined by McCaffrey equation for three zones axisymmetric buoyant plume as follows:

$\Delta T_0=2.94T_\infty$	when $\frac{z}{\dot{Q}^{2/5}}<0.08$	Continuous flame	(9)
$\Delta T_0=0.227T_\infty\left(\frac{\dot{Q}^{2/5}}{z}\right)$	when $0.08<\frac{z}{\dot{Q}^{2/5}}<0.2$	Intermittent flame	(10)
$\Delta T_0=0.076T_\infty\left(\frac{\dot{Q}^{2/5}}{z}\right)^{5/3}$	when $\frac{z}{\dot{Q}^{2/5}}>0.2$	Plume	(11)

And

$u_0=6.8z^{1/2}$	when $\frac{z}{\dot{Q}^{2/5}}<0.08$	Continuous flame	(12)
$u_0=1.9\dot{Q}^{1/5}$	when $0.08<\frac{z}{\dot{Q}^{2/5}}<0.2$	Intermittent flame	(13)
$u_0=1.1z^{-1/3}\dot{Q}^{1/3}$	when $\frac{z}{\dot{Q}^{2/5}}>0.2$	Plume	(14)

Where ΔT_0 = the different value between plume centerline temperature and ambient temperature (°C or K), u_0= ceiling jet velocity at plume centerline (m/s), $\dot{Q}$ = heat release rate (kW), T_∞ = Ambient temperature (°C or K), z = reference height (m)

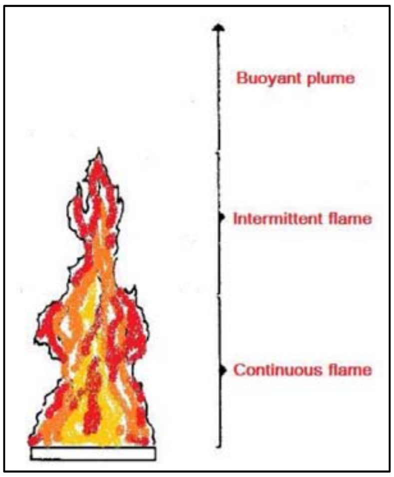

Figure 3 The three zones of the axisymmetric buoyant plume under McCaffrey theory (Sangkavorn and Chaengbamrung, 2017)

The amount of energy that produce from combustion of any material can be referred as heat release rate. Heat release rate is generally being as a function of the property of burning material such as heat of combustion Δh_c and burning area (A). (Bwalya et al.) expresses the heat release rate during growth stage by power law correlation or as follow:

$$\dot{Q}=\alpha t^p \qquad (15)$$

Where $\dot{Q}$= rate of heat release (kW), p = positive exponent (the exponent is given a value of 2 and hence format the curve as t-square fire as per NFPA 204 (2018)), t = time after effective ignition (s), α = fire growth coefficient (kW/s^2).

1.2 Fire dynamic simulation

Fire dynamic simulator (FDS) is a computational fluid dynamics (CFD) model of fire-driven fluid flow which currently developed by National Institute of Standards and Technology (NIST). As the scientific approach to help improve fire study, these tools is frequently use for visualize and explore solution on fire scenario. The application is of Large Eddy Simulation (LES) technique which solve numerically to a fire modeling. For instance, (The Fire Protection Research Foundation, 2008) carried out the modeling study for smoke detection performance for beamed ceiling. Variables are arranged and adjusted to define time activated of smoke-sensing device at given positions. Also, (Boonmee, 2007) has study the Large Eddy Simulation (LES) of smoke flow under beam ceiling for desired fire. The study has showed the confined ceiling jet temperature and velocity compared with Delichatsios's empirical correlation for multiple beam spacing to room height (W/H) and the beam depth to room height (h_b/H).

2. Objectives of the study

1. To study the sprinkler activation time impact by varying parameters of distance below ceiling, sprinkler response type index, and heat release rate of burning object.

2. To suggest the most responsiveness of sprinkler installation for waffle slab structure by the simulation result coupled with theoretical steady state ceiling jet behavior.

3. Materials and methods

In this study, the experiments were set in the simulation software and were divided into 2 major parts which consisted of the study of sprinkler activation time impact by distance below ceiling, response type index (RTI) and heat release rate of burning object for the first part. This is driven by using FDS, Pyrosim 2012 software. The second part is to analyze the ceiling jet characteristic and the most responsiveness of sprinkler from simulation output for design options.

The simulation is focused for studying sprinkler responsiveness in 16 scenarios as explained in Table 1:

Table 1 Fire simulation scenarios

Scenarios	Sprinkler RTI range ($m^{1/2}.s^{1/2}$)	Fire area (m^2)	Heat release rate per unit area (kW/m^2)	Sprinkler distance below ceiling (cm)
1	Fast response (50)	3	400	30, 96, 120
2			800	
3			1200	
4			1600	
5	Intermediate response (80)	3	400	30, 96, 120
6			800	
7			1200	
8			1600	
9	Lower-boundary standard response (100)	3	400	30, 96, 120
10			800	
11			1200	
12			1600	
13	Upper-boundary standard response (135)	3	400	30, 96, 120
14			800	
15			1200	
16			1600	

In fire modelling, the waffle slab is sketched as the same as actual site dimension which is distributed all over the boundary. The ceiling slab is concrete material. Fire mesh boundary is sized of 7.35 meters in width x 12.6 meters in length x 9 meters in height which equals to 92.61 m^2 in area. All four sides of boundary are open.The concrete tee is formed with 0.6 meters in width with 1.15-meter in depth vertically from the topmost ceiling. The room height is 9 meters. Each pocket has the same dimension of 3.4 meter in length and 1.65 in width opening. One fire sprinkler bulb is positioned in the center of each beam pocket. The sprinkler bulb is red-colored which fragile at 68 degrees Celsius. There are total of 9 ceiling pockets and 9 sprinkler heads in the simulation domain.

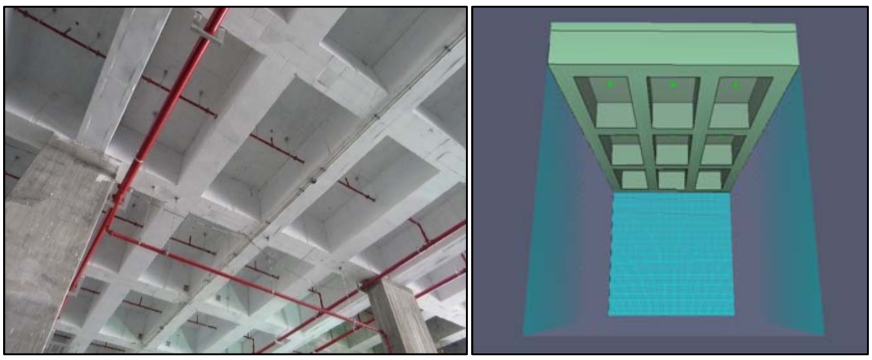

Figure 4 Actual site representing based-model for fire modelling and view from fire dynamic simulation

In this study, ceiling pocket location is simplified into reference number in "X*A*-Y*B*-DC*ZZ*" format. The numbering convention in this report would allow more efficient tracking and understanding of the result.

Where *"A"* is The waffle pocket number arranged in X-axis, which have number 1, 2, and 3.

"B" is The waffle pocket number arranged in Y-axis, which have number 1, 2, and 3.

"ZZ" is the sprinkler Distance Below Ceiling (DC) in centimeter unit. In this case the available numbers are only 30, 96, and 120 cm.

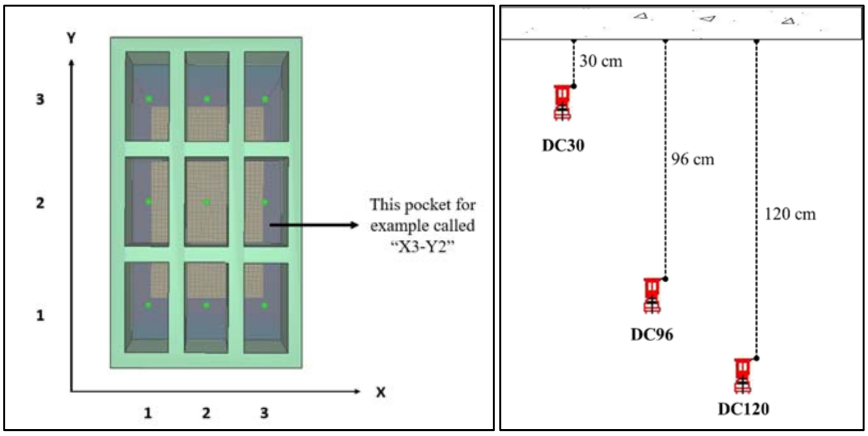

Figure 5 Number convention for waffle pockets and distance below ceiling (DC)

Apart from adding sprinkler head, the thermocouples and gas velocity devices are inserted at multiple radius (R) from the center of fire source as per Figure 6. They are used for gathering ceiling jet data and for comparing to empirical correlation to determine their characteristic.

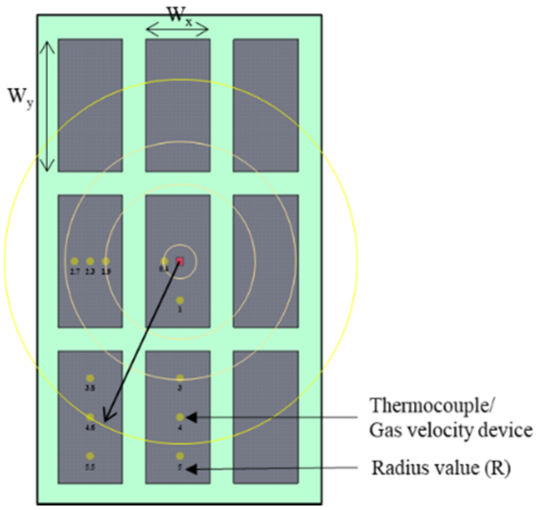

Figure 6 Fixed thermocouple/gas velocity device at multiple radius (R) in FDS simulation domain

4. Results and Discussions

There are four charts represented four (4) heat release rate simulations and each chart presented four (4) RTI values and three (3) sprinkler distance below ceiling (DC) variations. The output described the duration in seconds that the sprinkler heads were heated up and reach at activation point or 68 °C. There were some cases that sprinkler had not activated until termination of simulation at 600 seconds. The extracted simulation outcomes have shown in Figure 7-10. Sample of waffle pocket at location X1Y1, X1Y2, X2Y1, and X2Y2 had been addressed since they were a case of sprinkler presented at the corner, X-axis and Y-axis centers, and middle center of the domain.

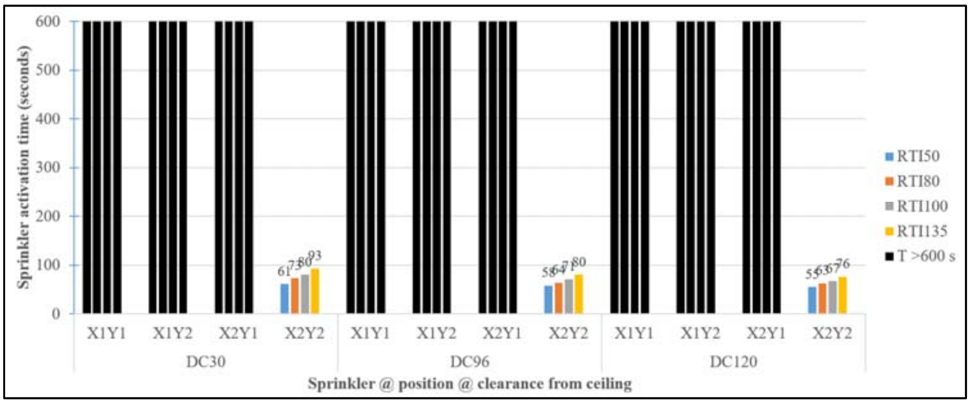

Figure 7 Sprinkler activation time at different position, RTI, and distance below ceiling (DC) for Heat Release Rate = 1,200 kW.

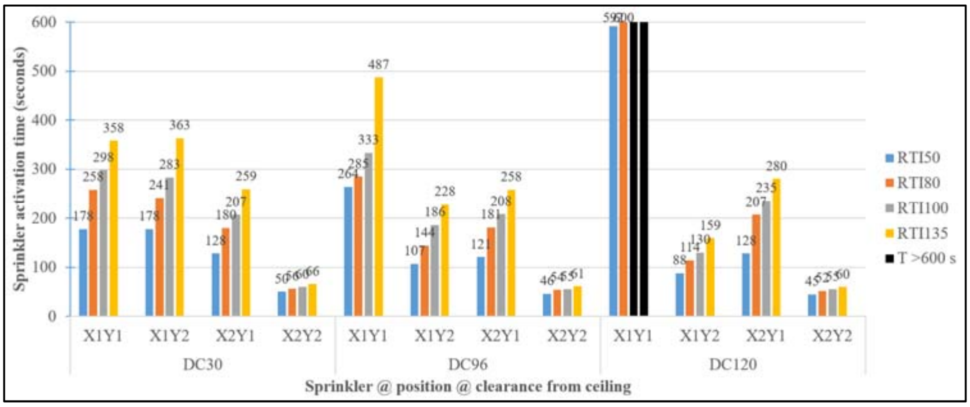

Figure 8 Sprinkler activation time at different position, RTI, and distance below ceiling (DC) for Heat Release Rate = 2,400 kW

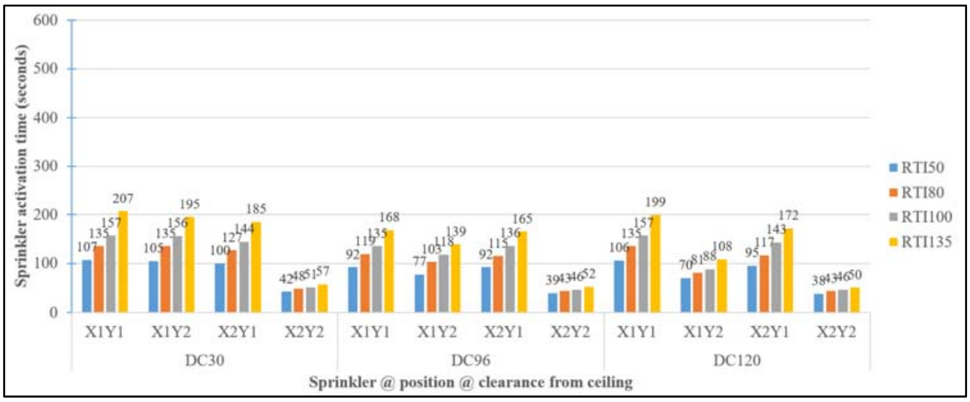

Figure 9 Sprinkler activation time at different position, RTI, and distance below ceiling (DC) for Heat Release Rate = 3,600 kW

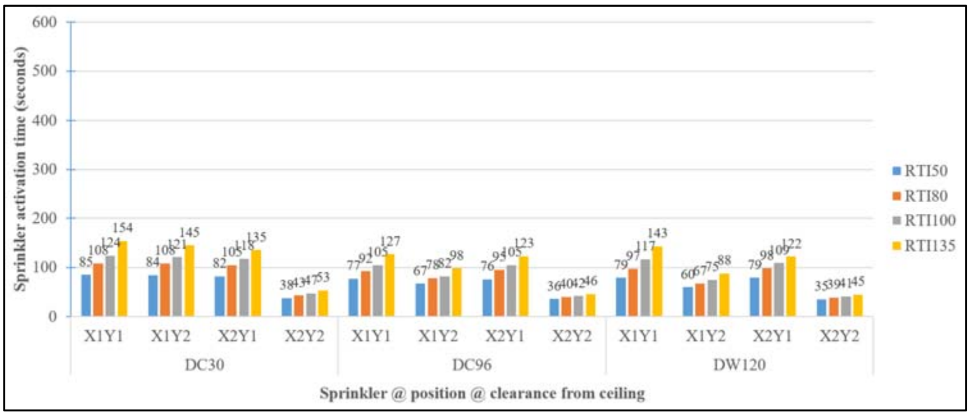

Figure 10 Sprinkler activation time at different position, RTI, and distance below ceiling (DC) for Heat Release Rate = 4,800 kW.

Table 2 The summary of sprinkler activation time and trend by varying factors.

No.	Variable factors	Change of factor	Sprinkler activation time trend	Value
1	Sprinkler response time index (RTI) ($m^{1/2}.s^{1/2}$)	Increasing 50 ⟶ 80 ⟶ 100 ⟶ 135	Increasing	6-100 seconds(1)
2	Sprinkler distance below ceiing (cm)	Increasing 30 ⟶ 96 ⟶ 120	Decreasing & Increasing	(-87)-600 seconds
3	Heat release rate (kW)	Increasing 1,200 ⟶ 2,400 ⟶ 3,600 ⟶ 4,800	Decreasing	4-507 seconds(2)

(1)Data from simulation at 3,600 kW

(2)Data from simulation with RTI50 sprinkler

From the result in Table 2, the value of sprinkler changes by distance below ceiling gave the most significant influence on the sprinkler activation time when comparing to RTI and heat release. Unfortunately, when heat release is lower than 1,200 kW, this limited heat energy was not able to trigger sprinkler at distance and thus presents the inactivated sprinkler heads until 600 seconds. The only activated sprinkler was the center pocket and in this case, fire could be retained by single sprinkler head.

From data collected via thermocouple and gas velocity device, the comparison of ceiling jet temperatures and velocity was plotted in graph and varied by R/H where ceiling height (H) is constant. The average trendline is created with general power equation. The ceiling jet temperature from simulation (T_{cj} Simulation) are represented in two conditions. One is the beam spacing width of 3.4 m (smoke spread along the X-Axis beam pocket or W/H = 0.39) and another for 1.65 m (smoke spread along the Y-Axis beam pocket or W/H = 0.19). Figure 11 shows the simulation result compared with Alpert's empirical correlation whereas Figure 12 is result compared with Delichatsios's empirical correlations at same heat release rate. Table 3 and 4 were the output summary from the result.

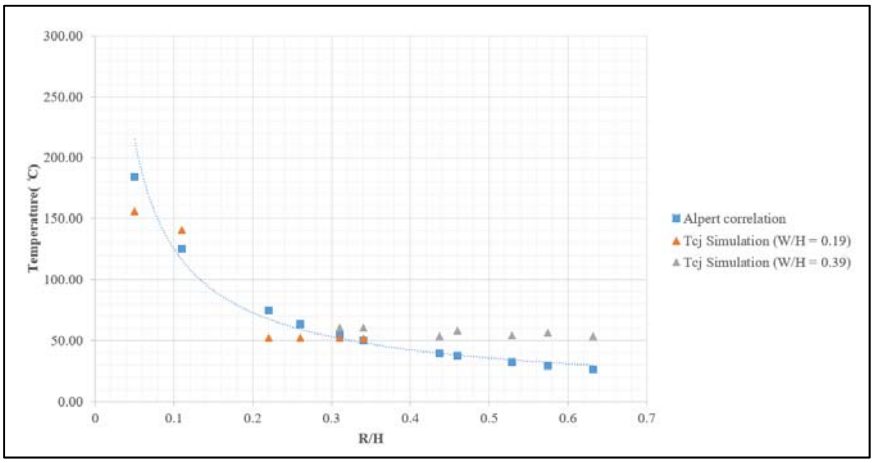

Figure 11 Ceiling jet temperature from simulation compare to Alpert's empirical correlation

(Heat release rate = 3,600 kW)

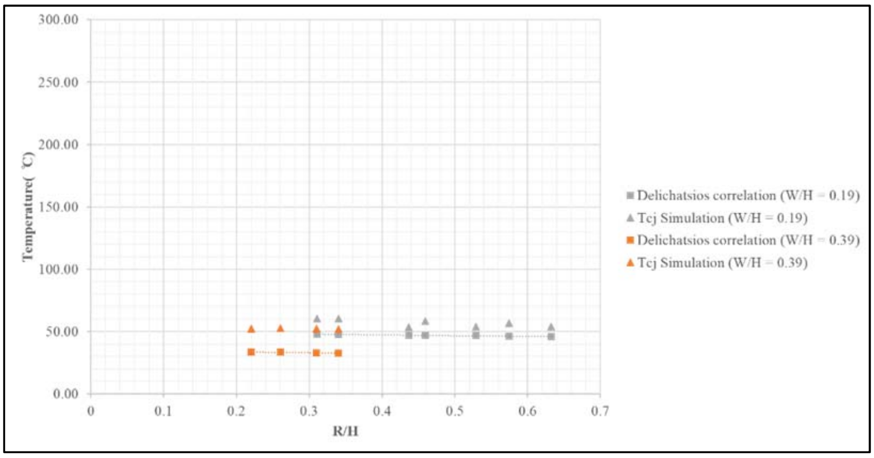

Figure 12 Ceiling jet temperature from simulation compare to Delichatsios's empirical correlation

(Heat release rate = 3,600 kW)

Table 3 Summary of ceiling jet assumption

Heat release rate (kW)	R/H	W/H	Average % Diff from Alpert's empirical correlation	Average % Diff from Delichatsios's empirical correlation	Ceiling jet likely being as
3.600	Up to 0.34	0.39	16.77	36.70	Unobstructed Ceiling jet
	> 0.34	0.19	32.28	19.62	Obstructed ceiling jet

Table 4 Screenshots of output on X-axis and Y-axis temperature plane over time (Heat release rate = 3,600 kW)

Screenshots of smokeview output on X-axis and Y-axis temperature plane		Time (Seconds)	Description
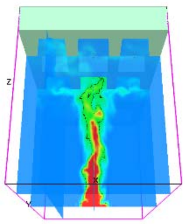	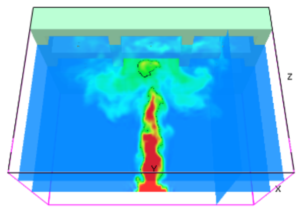	0-24	Fire ignited and gave off smoke. The plume hit the ceiling and start to spillover from the center pocket.
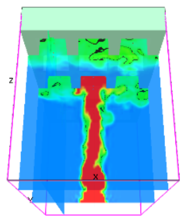	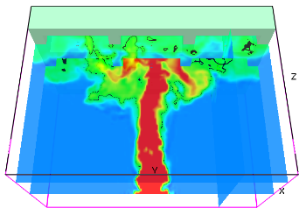	48	The hot air of $60-80^{\circ}C$ has spread to the side pockets and corner pockets. Less heat intense has been noted at the corner pockets when compared.
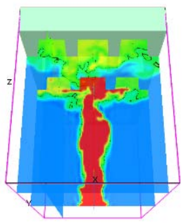	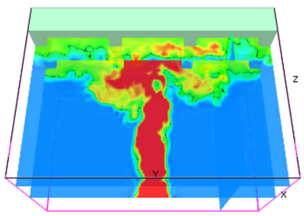	72	Smoke overwhelming all ceiling pockets and initially form a ceiling jet layer at the bottom of the tee construction. The temperature of ceiling jet is $60-120^{\circ}C$. The sprinkler at center pocket is already reach $68^{\circ}C$ and activated
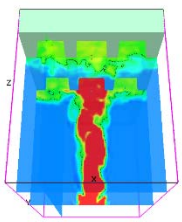	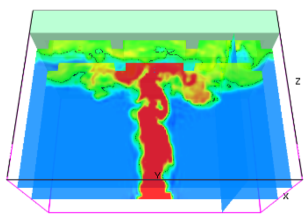	96	The corner pockets have completely filled with hot smoke. The ceiling jet temperature is in range of $60-120^{\circ}C$.
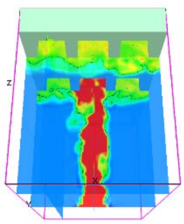	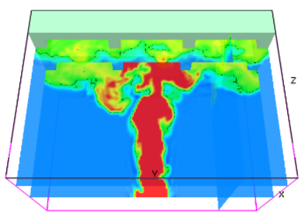	120	The smoke layer becomes more steady since heat release rate is steady

Despite the ceiling jet velocity (u_{cj}) part, the simulation result are also compared to theoretical correlation by Alpert and Delichatsios. The comparison of ceiling jet velocity is plotted as shown in Figure 13. From the simulation data, the ceiling jet behavior is obviously different from both correlation of Alpert and Delichatsios. At point of R/H > 0.11 or approximately 1 meter from the center of fire area, the velocity of ceiling jet is suddenly drop far below the theoretical value. This could be assumed that the limited volume of ceiling pocket has forced ceiling jet to spillover from the center pocket and formed thick smoke layer underneath tee stem as time passed.

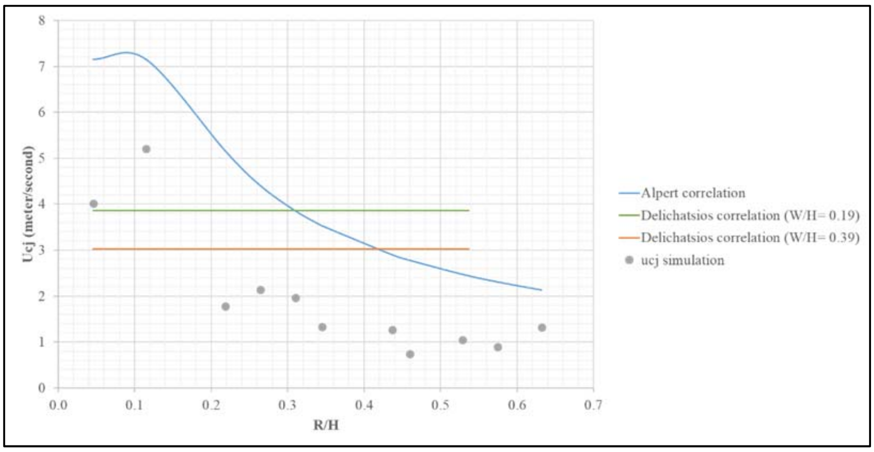

Figure 13 Gas velocity measured at different R/H at different ceiling clearance

Consider the gas velocity in different height layer, the ceiling jet has lower in velocity at near ceiling position and higher when closer to the bottom of concrete tee. The solid beam construction is presented as fixed obstruction to smoke spreading. For the fixed beam depth (h_b) and width (W) parameters shown in Table 5 and snapshots, the hypothesis is further explained that the gas velocity has similar characteristic for DC30 and DC96 which smoke cannot dissipate toward fixed obstruction and thus lower the value of gas velocity compared to both correlation of Alpert and Delichatsios.

Table 5 Simulation output of ceiling jet velocity over time

Screenshots of smokeview output with Z-axis velocity plane			**Time (Seconds)**	**Description**
Z-axis slice at DC30	**Z-axis slice at DC96**	**Z-axis slice at DC120**		
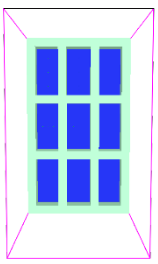	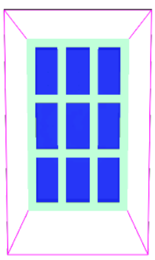	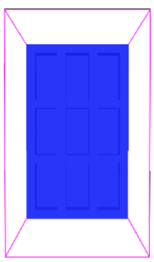	0-20	Fire ignited but smoke plume has not reach the ceiling. No gas velocity is captured at any slice layer.

Screenshots of smokeview output with Z-axis velocity plane			Time (Seconds)	Description
Z-axis slice at DC30	Z-axis slice at DC96	Z-axis slice at DC120		
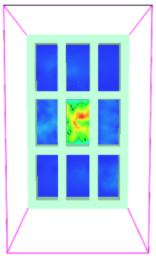	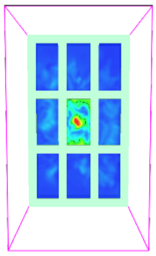	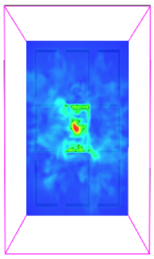	40	Plume velocity is peaked at center pocket. At DC96 and DC120, there is some increase in gas velocity at other ceiling pockets.
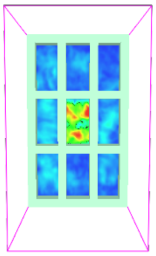	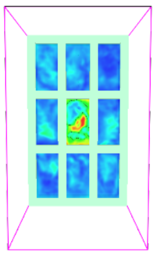	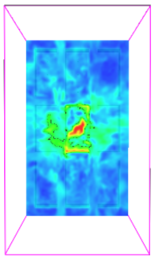	60	Heat release rate is at start point of fully developed fire. The layer DC120 or bottom of tee construction explicit widespread of higher in gas velocity. On the other side, ceiling pocket other than the center has low value at near ceiling level.
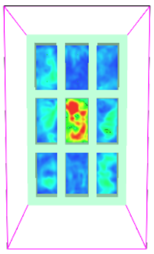	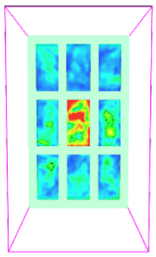	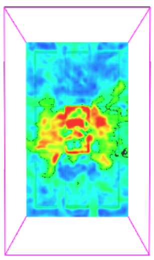	100	Smoke can freely spread at layer DC120 and it could develop into thick ceiling jet later under the tee. At DC30, the beam construction has blocked high velocity gas in center pocket.
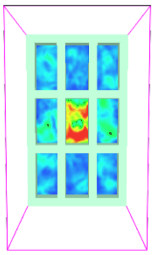	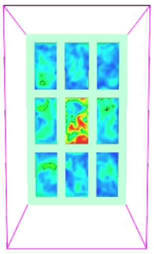	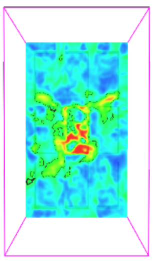	200	At steady state, the velocity is maximum at 7-8 m/s at center pocket while the others has a maximum gas velocity of 3 m/s.

5. Conclusion

In conclusion, the study can summarize into the followings.

1. The smaller sprinkler RTI chosen, the faster sprinkler activates at all cases.

2. The increase of sprinkler distance below ceiling is dependent to the heat release rate. The sprinkler can either activate faster or slower by this change. The sprinkler head not located directly above burning area will

activate slower when increase sprinkler distance below ceiling. This occurs for steady state fire with heat release rate of 2,400 kW and below.

3. The higher of heat release rate, the faster sprinkler activates.

4. The ceiling jet behavior is determined by ceiling jet temperature data as unobstructed ceiling jet where W/H = 0.39 and R/H < 0.34 whereas considered as obstructed ceiling jet where W/H = 0.19 and R/H > 0.34 by this simulation domain. The ceiling jet behavior is of obstruction ceiling jet at R/H > 0.11 or approximately 1 meter from the center of fire area by gas velocity.

5. The most responsiveness of sprinkler installation is to apply the smallest RTI50 sprinkler and installed at distance below ceiling of 30 cm to ensure sprinkler activation at sufficient heat release rate. The second option is to allow sprinkler delay in activation for 135 seconds by install any RTI sprinkler at distance below ceiling of 96 cm which fulfill the obstruction to sprinkler discharge pattern development and still conform to NFPA standard.

The researcher suggestions for further research are as follows:

1. Further study the effect of waffle beam in different depth and beam span is recommended. This study is limited to the defined beam characteristics so smoke dispersion would be more different if the parameter changes.

2. The domain of ceiling pocket is fixed with 9 pocket ceilings. It is recommended that it can be expanded in bigger spacing to study the effect of ceiling jet and temperature at different radius.

References

Boonmee, N. (2016). *Fire Dynamics*. Kasetsart University, Bangkok, Thailand

Boonmee, N. (2007). *A Numerical Investigation of Smoke Flow under Beamed Ceiling***.** The 21st Conference of the Mechanical Engineering Network of Thailand (pp. 921-926), Thailand.

Dyer, J.W. (2008). *Effectiveness of Automatic Fire Sprinklers in High Ceiling Areas & the Impact of Sprinkler Skipping.* M.S. Thesis, University of Canterbury.

Evans, David D. SFPE Handbook of Fire Protection Engineering, Chapter 4, Section 2. *Ceiling Jet Flows***.**

Fire Protection Research Foundation. (2008). *Smoke Detector Spacing Requirements Complex Beamed and Sloped Ceilings*, Volume 2. Massachusetts, U.S.A.

Johansson, N., Wahlqvist, J., and Van Hees, P. (2013). *Simple Ceiling Jet Correlation Derived from Numerical Experiments***.** Interscience Communications.

National Fire Protection Association 204. (2018). *Standard for Smoke and Heat Venting*.

Sangvakorn, V. and Chaengbamrung, A. (2017). *A Study of The Effect of Position Level on Heat and Smoke Detector Performance by Computational Fluid Dynamics***.** The 31st Conference of the Mechanical Engineering Network of Thailand, Thailand.